전력전자학술대회 논문집 2003. 7. 14 ~ 7. 17

Cooling System Design in Power Electronic

Chan-Ki Kim*, Hong-Woo Rhew*, Yoon-Ho Kim, and J. Holtz*****
*KEPRI, **Chung-ang Univ, ***Wuppertral Univ

ABSTRACT-In this paper, heatsink design for high power converter is presented. There are many ways of designing heatsink, but air cooling is by far the most used and much more practical than any of the other methods. In this paper, the practical methods of cooling which include the method to reduce a noise and a vibration due to a fan and the method to design a gap resistance and a contact resistance due to mounting force between thyristor and heatsink is proposed. Finally, simulation and experimental results are described to verify validity of the proposed method.

1. Introduction

Electronic power conversion equipment relies on the flow and control of electrical current to perform its task. Whenever electrical current flows through electronic component parts, heat is generated by the flow of electrical current in electronic component parts such as resistors, diodes, transistors, and transformers - most of the parts found in a typical power converter shown in Figure 1. Heat always flows from the hot area to the cool area.

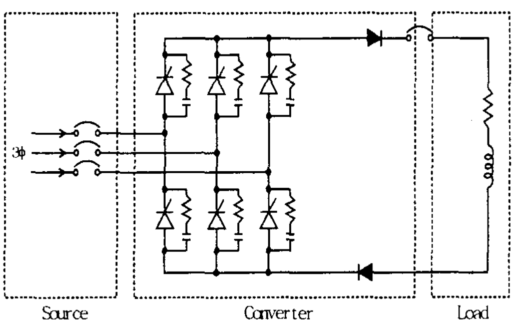

Fig. 1 Diagram of High Power Converter

There are three basic methods by which heat can be transferred: radiation, conduction, and convection. Fig. 2 shows the thermal equivalent circuit of a thyristor mounted on a heat sink. For sustained power dissipation Q at the junction, the junction temperature

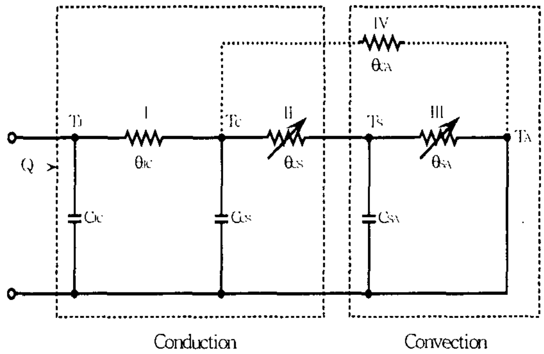

Fig. 2 Thermal equivalent circuit of a thyristor mounted on a heatsink.

T_J can be calculated as:

$$T_J - T_A = Q(\theta_{JC} + \theta_{CS} + \theta_{SA}) \quad (1)$$

$$\theta_{JC} = \frac{L_1}{k_1 A_{JC}\eta_1} \quad (2)$$

$$\theta_{CS} = \frac{L_2}{k_2 A_{CS}\eta_2} \quad (3)$$

$$\theta_{SA} = \frac{1}{h_c A_{SA}\eta_3} \quad (4)$$

In equation (1), (2), (3) and (4), T_A and T_J is the ambient temperature and junction temperature and A_{JC}, A_{CS} and A_{SA} represent a contact surface from junction to case, case to heatsink and sink to ambient, and sink to ambient, respectively. L_1 and L_2, represent a thickness from junction to case, case to heatsink. η_1, η_2 and η_3 is the efficiency of θ_{JC}, θ_{CS} and θ_{SA}. the h_c is the coefficient of convection heat transfer. k_1 is the thermal conductivity from junction to case, k_2 is the thermal conductivity from case to heatsink.

3. Heatsink Design Viewpoint from Noise & Vibration

Air forced cooling method can cause the noise and vibration due to a fan. A big noise reduces the commercial value of products and a critical vibration can cause thyristor failure directly. Therefore, a noise and a vibration due to fan have to be considered in case of designing air-forced cooling method

Firstly, noises of heat sink consist of air-borne noise, structure-borne noise and pipe resonance. The air-borne noise is the noise of fan itself, structure-borne noise is the heat sink noise caused by fan vibration and pipe resonance noise is the noise that the fan noise is amplified by the air duct of heat sink. Figure 3 shows the theory of heat sink noise according to heat sink structure.

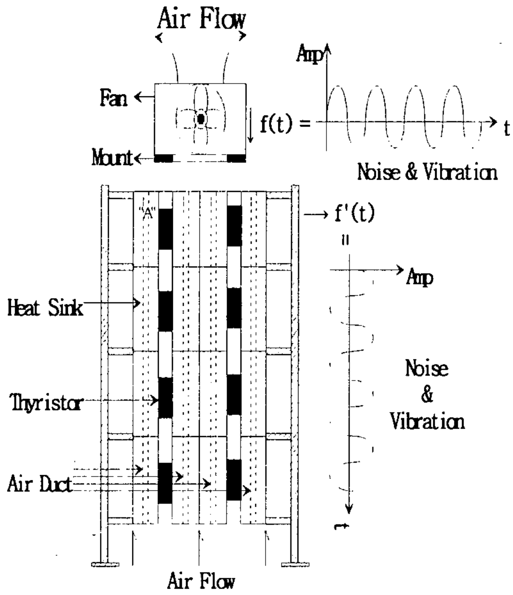

Fig. 3 Heat sink construction

3.1 Air-borne noise

The noise frequency of air-borne noise is following as :

$$f_b = \frac{BkadeNum. \cdot BladeRPM}{60Hz} \quad (5)$$

3.2 Pipe resonance

The equ. (6) shows the pipe resonance frequency.

$$f_p = \frac{C}{2 \cdot l} \quad (6)$$

where, C is 343m/sec and l is the length of pipe

3.3 Structure-bone noise

A mass, a spring constant and a damping constant between fan and heat sink determine structure-borne noise. Therefore, if the spring constant is changed, the noise can be reduced. The natural frequency of the heat sink is following as :

$$f_r = \frac{1}{2\pi} \cdot \sqrt{\frac{k}{M}} \quad (7)$$

where, k is spring constant, M is total fan mass.

The equation (8) shows the design method of a spring constant, the equation of transfer rate (T_r) is following as :

$$T_r = \frac{\sqrt{1 + [2 \cdot \zeta \cdot (\frac{w}{w_n})]^2}}{\sqrt{[1 - (\frac{w}{w_n})]^2 + [2 \cdot \zeta \cdot (\frac{w}{w_n})]^2}} \quad (8)$$

where, $\zeta = \frac{C_e}{2 \cdot \sqrt{k \cdot m}}$, $w_n = \sqrt{\frac{k}{m}}$

w = Forced Excitation Frequency

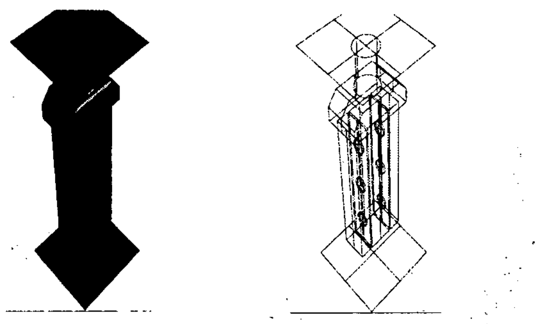
Fig. 4 External form of heatsink

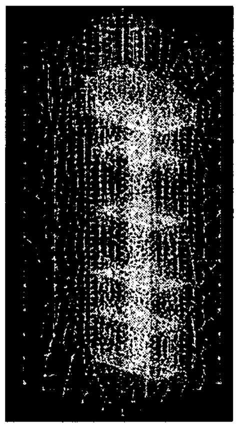
Fig. 5 Analysis model of heatsink

Fig. 4~8 drawn using an analytic heat transfer code, FLUENT, show the results of theheat distribution of heat sink. Fig. 4 shows the analytic model of heat sink, the analytic model used unstructured grid and one hundred thousand cells and symmetry plane. To simulate the convection due to airflow, the following was considered in a turbulent flow model :

- the case with fan is standard k-e
- the case without fan is laminar

Fig. 5 shows the analysis results for heat sink with 2 fans at environment temperature 20 degree.

Fig. 6 is simulated in the case of outage of fan 1 and fig. 7 is without fan. Finally, fig. 8 is the result of the case without fan and environment temperature 50. Fig. 9 shows an experimental set that measures resistances according to changes of pressure or contact resistance of the thyristor. An experimental heat sink system used in this paper is shown in Fig. 10. The second fan was designed for a use of emergency backups.

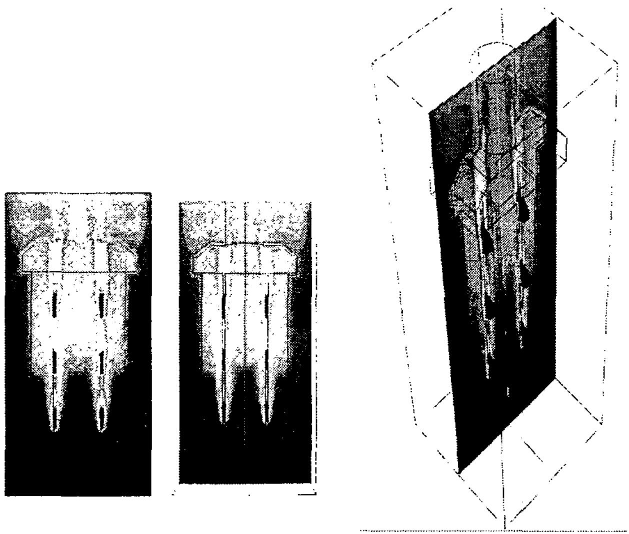

a) Temperature distribution b) Three-dimensional temperature distribution

Fig. 6 Temperature distribution of heatsink
(environment temperature : 20℃, with 2 fans)

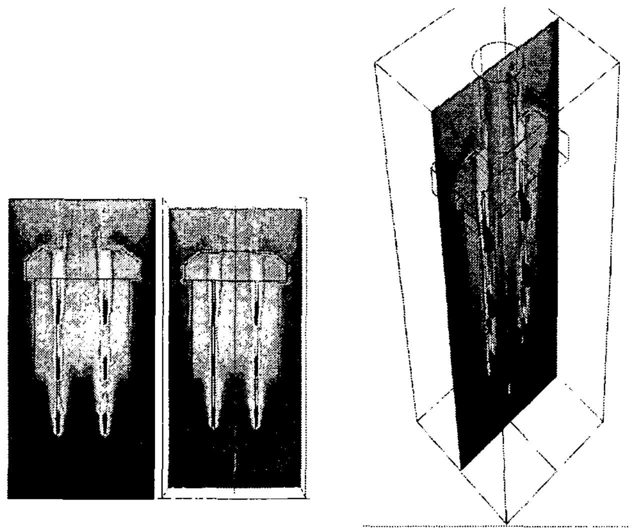

a) Temperature distribution b) Three-dimensional temperature distribution

Fig. 7 Temperature distribution of heatsink
(environment temperature : 20℃, with 1 fac)

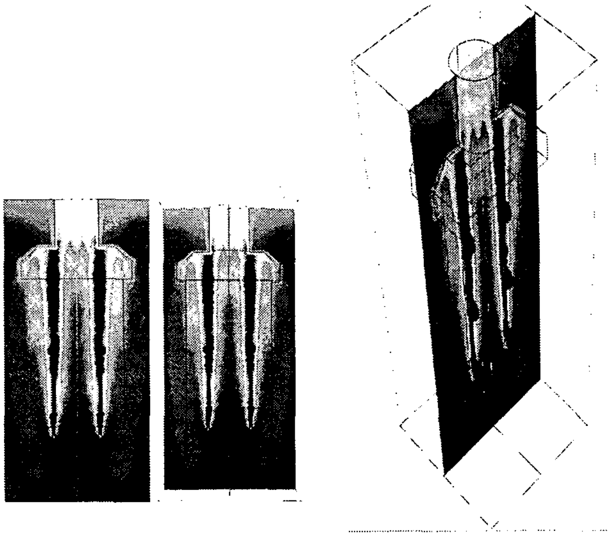

a) Temperature distribution b) Three-dimensional temperature distribution

Fig. 8 Temperature distribution of heatsink
(environment temperature : 20℃, without fan)

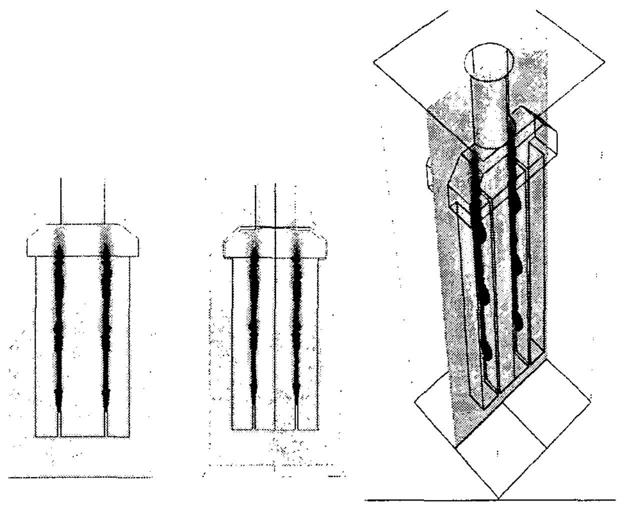

a) Temperature distribution b) Three-dimensional temperature distribution

Fig. 9 Temperature distribution of heatsink
(environment temperature : 50℃, without fan)

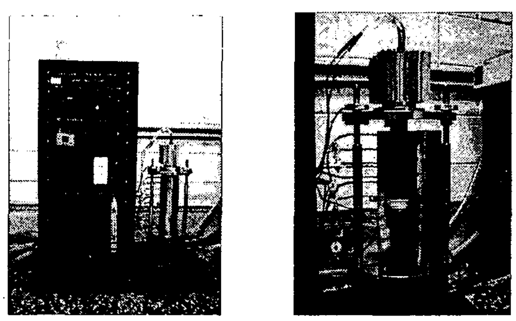

a) b)

Fig. 10 Thermal resistance experimental set

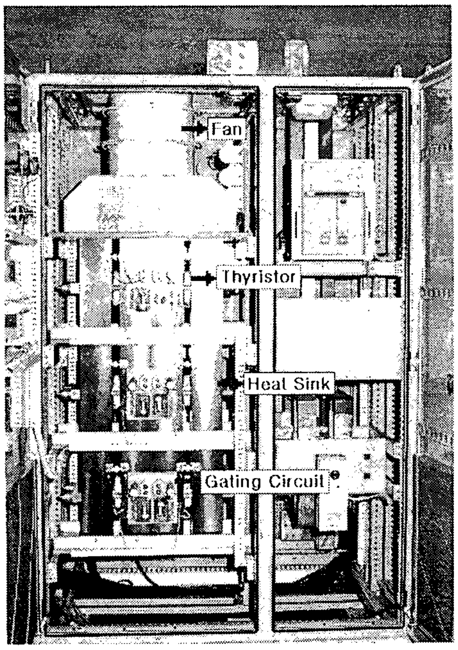

a) Front of the converter

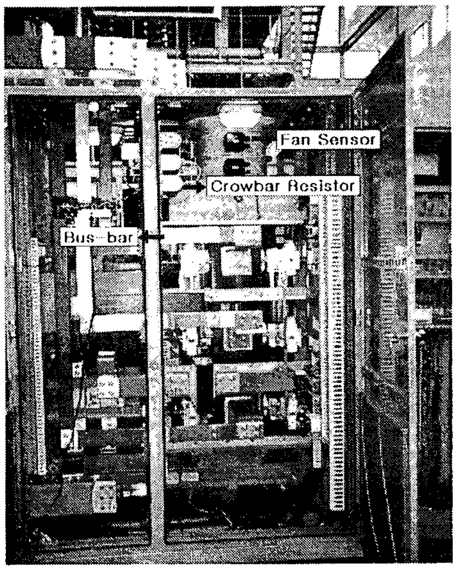

b) Back of the converter

Fig. 11 Implemented heatsink of high power converter

5. CONCLUSION

An efficiency heatsink system has been developed. The conventional heatsink has been replaced with efficiency heatsink system including a contact resistance and a gap resistance, eliminating a noise and vibration of a fan for heatsink. Also, the proposed method in this paper can be applied to IGBT, GTO converter. Finally, the detail design methods and experimental results including field test results will be presented in the final paper.

REFERENCE

[1] Cooper, M.G., Mikic, B.B. and Yovanovich M.M., "Thermal Contact Conductances", International Journal of Heat and Mass Transfer, Vol. 12, pp. 279-300, 1969.

[2] Yovonovich, M.M., "Thermal Contact Correlations", "Spacecraft Radiative Transfer and Temperature Control" Edited by T.E. Horton, Vol. 83 of Progress in Astronautics and Aeronautics, New York, 1982.

[3] De Vaal, J.W., Yovanovich, M.M. and Negus, K.J., "The Effect of Surface Slope Anisotropy on the Contact Conductances of Conforming Rough Surfaces", "Fundamentals of Conduction and Recent Development in Contact Resistance, ASME HTD-Vol. 69, pp. 123-134., 1987.

[4] Song, S and Yovanovich, M.M.,"Relative Contact Pressure Dependence on Surface Roughness and Vickers Microhardness", AIAA Journal of Thermophysics and Heat Transfer, Vol. 2, No. 1, pp. 43-47, 1988.

[5] D. Finney, "The Power Thyristor and its Applications", McGraw-Hill, 1980.

[6] A.F. Mills, "Heat Transfer", Richard D. IRWIN, INC., 1992.

[7] Thyristor Data Book, ABB INC. 1995.

[8] M. Necati ozisik, "Heat Transfer-a Basic Approach", McGraw-Hill, 1981.